Task Switching in Traumatic Brain Injury Relates to Cortico-Subcortical Integrity

Inge Leunissen,[1]* James P. Coxon,[2] Karen Caeyenberghs,[1] Karla Michiels,[3] Stefan Sunaert,[4] and Stephan P. Swinnen[1]

[1]*Movement Control and Neuroplasticity Research Group, Department of Kinesiology, Group Biomedical Sciences, KU Leuven*
[2]*Movement Neuroscience Laboratory, Department of Sport and Exercise Science, University of Auckland, New Zealand*
[3]*Department of Physical Medicine and Rehabilitation, University Hospital, Leuven Campus Pellenberg, Belgium*
[4]*Medical Imaging Research Center, Group Biomedical Sciences, KU Leuven, Belgium*

Abstract: Suppressing and flexibly adapting actions are a critical part of our daily behavioral repertoire. Traumatic brain injury (TBI) patients show clear impairments in this type of action control; however, the underlying mechanisms are poorly understood. Here, we tested whether white matter integrity of cortico-subcortical pathways could account for impairments in task switching, an important component of executive functioning. Twenty young adults with TBI and eighteen controls performed a switching task requiring attention to global versus local stimulus features. Diffusion weighted images were acquired and whole brain tract-based spatial statistics (TBSS) were used to explore where white matter damage was associated with switching impairment. A crossing fiber model and probabilistic tractography further identified the specific fiber populations. Relative to controls, patients with a history of TBI had a higher switch cost and were less accurate. The TBI group showed a widespread decline in fractional anisotropy (FA) throughout the TBSS skeleton. FA in the superior corona radiata showed a negative relationship with switch cost. More specifically, this involved cortico-subcortical loops with the (pre-)supplementary motor area and superior frontal gyrus. These findings provide evidence for damage to frontal-subcortical projections in TBI, which is associated with task switching impairments. *Hum Brain Mapp 00:000–000, 2013.* © **2013 Wiley Periodicals, Inc.**

Key words: traumatic brain injury; executive function; basal ganglia; diffusion tensor imaging

INTRODUCTION

In Europe, the incidence of traumatic brain injury (TBI) is estimated at 235 per 100,000, with an average mortality of about 15 per 100,000 [Tagliaferri et al., 2006]. Of those who survive, a large proportion suffers from chronic executive dysfunction [Colantonio et al., 2004; Draper and Ponsford, 2008]. TBI patients show clear impairments in

Additional Supporting Information may be found in the online version of this article.

Contract grant sponsor: Research Program of the Research Foundation—Flanders (FWO); Contract grant number: G.0483.10; Levenslijn G.0482.10; and G.A114.11; Contract grant sponsor: Interuniversity Attraction Poles program of the Belgian federal government [P7/11]; Contract grant sponsor: PhD fellowship of the Research Foundation—Flanders (FWO).

*Correspondence to: Inge Leunissen, Tervuursevest 101, B-3001 Heverlee, Belgium. E-mail: inge.leunissen@faber.kuleuven.be

Received for publication 22 October 2012; Revised 15 May 2013; Accepted 19 May 2013.
DOI 10.1002/hbm.22341
Published online in Wiley Online Library (wileyonlinelibrary.com).

the suppression and flexible adaptation of actions [Larson et al., 2006; Leunissen et al., 2013], which are hallmarks of executive function.

Executive dysfunction is traditionally associated with frontal lobe lesions [Bianchi, 1985], and is therefore even referred to as a frontal lobe syndrome. In TBI frontal lobe contusions are common, but their location and extent often cannot fully explain the patient's impairments [Bigler, 2001]. Dysexecutive behavior has also been reported in patients with lesions outside the frontal lobe [Bhatia and Marsden 1994; Levy and Dubois 2006; Krause et al., 2012], and most of these lesions were reported in the basal ganglia (BG) and thalamus. Moreover, neuropsychological studies in patients with Parkinson's and Huntington's disease have shown that the BG are essential in executive functioning [Taylor and Saintcyr 1995; Brandt and Butters 1996].

Traumatic impact also causes movement of the brain relative to the skull, resulting in diffuse axonal injury (DAI) of white matter connections between the frontal cortex and subcortical circuitry such as the BG, thalamus, and cerebellum [Gentry et al., 1988; Zappala et al., 2012]. DAI is a progressive process, from focal axonal alteration to ultimate disconnection [Buki and Povlishock, 2006], evident in all severities of TBI and is likely a major cause of impairment [Wallesch et al., 2001a, b]. Unfortunately, conventional CT and MRI underestimate the extent of DAI after TBI [Rugg-Gunn et al., 2001; Arfanakis et al., 2002]. On gradient-echo images one can identify microbleeds, which are a marker of DAI [Scheid et al., 2003], but patients without microbleeds can still show significant white matter abnormalities [Kinnunen et al., 2011].

Diffusion tensor imaging (DTI) provides a validated and sensitive way of identifying the impact of DAI [Mac Donald et al., 2007]. DTI measures the directionality of water diffusion, which gives information about the microstructural organization of the white matter bundles [Basser, 1995; Tournier et al., 2011]. From this, metrics such as fractional anisotropy (FA) can be derived to quantify the degree of white matter disruption. High FA values are believed to reflect more coherent tissue structure, whilst increased diffusivity, resulting in lower FA, suggests tissue damage.

The relationship between executive dysfunction after TBI and white matter damage has been established in previous studies [Kraus et al., 2007; Niogi et al., 2008; Little et al., 2010; Kinnunen et al., 2011; Newcombe et al., 2011]. However, these studies have mainly focused on frontal white matter and made use of general clinical assessments of executive function. Behavioral studies have shown that deficits in executive function in TBI are particularly evident in situations where response conflict is high, and when inappropriate prepotent response tendencies have to be overcome [Mecklinger et al., 1999; Levin et al., 2004; Seignourel et al., 2005; Larson et al., 2006; Perlstein et al., 2006]. Therefore we made use of a local-global task switching paradigm which requires a high degree of flexible cognitive control over action. The presence of conflict creates conditions in which the executive demands can be increased (switch trials) or reduced (repeat trials). Accumulating evidence suggests that behavioral switching is mediated by interactions between the supplementary motor complex (SMC) and subcortical structures [Mink, 1996; Nambu et al., 2002; Rushworth et al., 2004; Nachev et al., 2008; Hikosaka and Isoda, 2010]. The SMC links situations with appropriate actions (Nachev et al., 2008), and the BG influence action selection via pathways which serve to focus thalamo-cortical output [Mink, 1996; Hikosaka and Isoda, 2010].

Moreover, previous DTI studies suffer from serious limitations in regions of crossing fibers because traditional tensor techniques cannot represent multiple, independent intravoxel orientations [Behrens et al., 2007], possibly concealing subcortical involvement. A model that takes crossing fibers into account can enhance interpretability because it provides more tract specific information [Jbabdi et al., 2010]. Therefore, we made use of such a crossing fiber model to test the hypothesis that patients with the most extensive damage to frontal-subcortical fibers would perform worst on an experimental task requiring cognitive control over action.

METHODS

Participants

Twenty patients with a history of traumatic brain injury (mean age 24.7, range 16–34, 14 male) and eighteen healthy volunteers (mean age 25.1, range 21–28, 9 male) were recruited. The groups did not differ significantly with respect to age ($t(36) = -0.29$, $P = 0.77$) or gender ($\text{Chi}^2 = 1.59$, $P = 0.21$). All TBI patients were assessed at least 6 months postinjury. Injuries were secondary to traffic accidents ($N = 19$) or falls ($N = 1$). Average time since injury was 4.1 years (range 1–10; SD 2.8) and age at injury was 20.7 years (range 9–29; SD 5.7). According to the Mayo classification system for injury severity, our TBI group consisted of moderate-severe patients. This system grades patients according to duration of loss of consciousness (LOC), length of post-traumatic amnesia (PTA), lowest recorded Glasgow Coma Scale in the first 24 h, and initial CT or MRI images [Malec et al., 2007]. LOC was on average 16.7 days (range 0.014–30; SD 9.7), PTA was on average 22.8 days (range 0.042–38; SD 10.9). All patients showed evidence of contusions, microbleeds, or both on their initial CT or MRI scans. A neuroradiologist (S.S.) assessed all T_1-weigthed structural images and gradient-echo images. Ten patients showed residual evidence of contusions; of these, five also had evidence of microbleeds. A further nine patients only showed evidence of microbleeds. For the remaining patient there were no apparent abnormalities. Contusions were typically situated in the inferior parts of the frontal lobes, including the orbitofrontal cortex, and the temporal poles [Gentry et al., 1988]

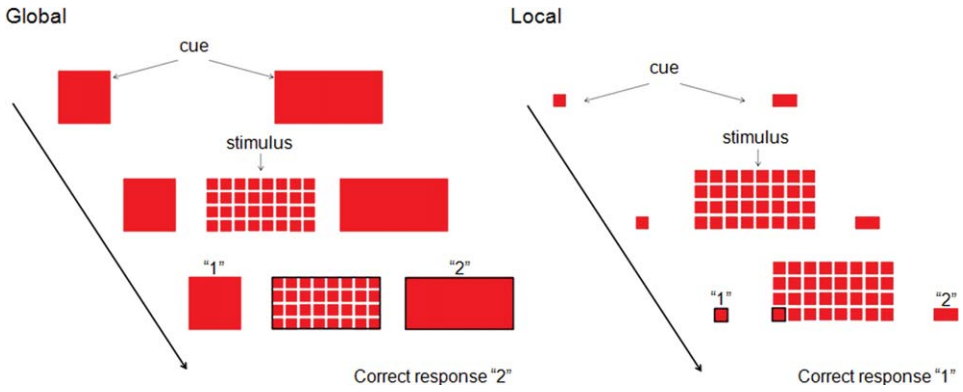

Figure 1.
Local-global task. Each trial started with a cue, indicating whether attention had to be paid to the global or local level. When the stimulus appeared subjects had to rapidly decide whether the relevant level consisted of squares or rectangles. They should press key "1" with their index finger for squares and key "2" with their middle finger for rectangles.

(Supporting Information Table SI, Supporting Information Fig. S1).

All participants were right-handed (laterality quotient: *TBI*: mean 81.5; SD 19.8 *Controls*: mean 93.7; SD 12.8) [Oldfield, 1971]. The study was approved by the local ethics committee, and the subject or caregiver (when <18) provided written informed consent.

Local-Global Task

The local-global task refers to the concept of task switching, which is considered one of the different manifestations of executive function. This is relevant in daily life, in which we often have to make flexible switches between tasks. The task has been used as a research tool to investigate the ability to suppress attention to the more salient aspects of perceptual displays [Navon, 1977]. To use the set of executive control components identified by Miyake et al. [2000], the task requires inhibition (ignore misleading cues), updating (monitor display in the context of current instructions), and switching (adjusting response according to current rule). Moreover, the presence of conflict creates conditions in which the executive demands can be increased (switch trials) or reduced (repeat trials).

Participants performed the local-global task with their right hand. The target stimulus (as shown in Fig. 1) consisted of a "global" square or rectangle, composed of much smaller "local" squares or rectangles. Each trial began with the presentation of a prime cue, indicating the dimension to attend to. The global dimension was cued by a big square, to the left of the stimulus, and a big rectangle to the right. For the local dimension a small square and rectangle appeared. After a random cue-target interval of 400–600 ms, the target stimulus was presented. Both the prime cue and the target stimulus remained on the screen until the participant responded, or until 2,500 ms had elapsed. Participants were required to identify the relevant target stimulus dimension and press "1" with their index finger for squares and "2" with their middle finger for rectangles (Fig. 1). The interval between a response and the presentation of the next trial varied randomly between 900 and 1,100 ms.

The experiment was comprised of two unidimensional blocks, and one switch block. In one of the unidimensional blocks, participants attended to only the global cues, and in the other to the local cues. The order was counterbalanced across participants. In the third switch block, the target stimulus dimension alternated every other trial (i.e., two "local" trials, followed by two "global" trials, etc.). When the prime cues changed, the participants had to switch from responding to the local dimension to the global dimension, and vice versa. A short amount of practice was given to ensure the instructions were understood (four trials for each unidimensional block, and 8–16 trials for the switch block). The experiment consisted of 24 trials in each unidimensional block, and 49 trials in the switch block. Differences in switch cost (reaction time switch trials—reaction time repeat trials) and switch accuracy were tested with two-tailed Student t tests, using a statistical threshold of $P < 0.05$ (Statistica 8, StatSoft, Tulsa, OK).

MRI Data Acquisition

A Siemens 3 T Magnetom Trio MRI scanner (Siemens, Erlangen, Germany) with an eight channel head coil was used for acquisition of a high resolution T_1-weighted structural image [MPRAGE; TR = 2,300 m, echo time (TE) = 2.98 ms, 1.1 × 1 × 1 mm^3 voxels, field of view (FOV): 240 × 256, 160 sagittal slices], gradient echo images were acquired with a gradient echo planar imaging (EPI) pulse sequence for T_2^*-weighted images (TR = 3,000 ms, TE = 30 ms, flip angle = 90°, 50 oblique axial slices each

2.8-mm thick, interslice gap .28 mm, in-plane resolution 2.5 × 2.5 mm^2, 80 × 80 matrix), and single shot spin-echo diffusion weighted images (TR = 7,200 ms, TE = 81 ms, 56 sagittal 2.2-mm slices with 0.66-mm gap, in plane resolution 2.19 × 2.19 mm, matrix 96 × 96) with diffusion sensitizing gradients applied along 64 noncollinear directions (b-value of 1,000 s/mm^2). In addition, one image with no diffusion weighting (b_0) was acquired.

DTI Processing

Diffusion data were preprocessed and analyzed using FMRIB Software Library (FSL) version 4.1. First, the b_0 image of each subject was skull-stripped using the brain extraction tool, the data was corrected for subject motion and eddy-current induced geometrical distortions, and the diffusion sensitizing gradients ("bvecs") were rotated to correct for motion. Using the FSL Diffusion Toolbox, the diffusion tensor model was fit to the data, from which fractional anisotropy images (FA) were calculated.

For voxel-based analyses of white matter structure across the whole brain we used tract-based spatial statistics (TBSS). This method restricts analysis to a FA skeleton onto which the central white matter tract values for each subject is projected. This approach is robust to systematic group differences, such as brain atrophy and allows for more sensitive statistical testing and objective interpretation of the results [Smith et al., 2006]. First, all subjects' FA data was registered to a common space (the FA158 MNI space template) using a combination of affine and nonlinear registration. A mean FA image was created, eroded to a skeleton and thresholded at FA > 0.25. Each subject's aligned FA data was then projected onto this skeleton and used for voxelwise statistical analysis (Randomize, 10,000 permutations). The contrasts comparing TBI versus Controls were cluster thresholded with a cluster forming threshold of $t > 3.6$, resembling a two-tailed statistical threshold of $P < 0.001$. The 95th percentile was then used as cluster-size threshold, i.e. clusters were thresholded at $P < 0.05$, fully corrected for multiple comparisons across space [Jbabdi et al., 2010]. For correlations between switch cost and switch accuracy and FA we grouped the TBI and control subjects together, adding age as a covariate of no interest. For switch cost we wanted to minimize the potential effect of processing speed, therefore we added average RT of the two unidimensional (non-switch) blocks as an extra covariate. Inference was carried out using the same cluster thresholding procedure.

An important limitation of the tensor model is that it assumes that water self-diffusion has a Gaussian diffusion profile. This assumption is quite accurate when there is only one white matter tract present in a certain voxel, but fails to resemble the microarchitecture in the presence of crossing fibers [Behrens et al., 2007; Jbabdi et al., 2010]. The significant cluster from our whole-brain FA correlation analysis occurred in a region of crossing fibers. We therefore made use of a crossing fiber model (BEDPOSTX) to resolve which fiber population was driving the effect. This probabilistic diffusion model calculates probability distributions on fiber direction at each voxel in subject diffusion space, allowing for estimates of more than one fiber direction within a voxel [Behrens et al., 2003, 2007]. Specifically, the contribution of major (f_1) and secondary (f_2) fiber directions are calculated for each voxel. These scalar values were reassigned to obtain a consistent labeling within and across subjects [Jbabdi et al., 2010]. The resulting partial volume fractions (f_1 and f_2) were used for TBSS, with switch cost and age as covariates. The significant cluster from the whole-brain FA correlation was used as a ROI mask, therefore inference was carried out at the voxel level with correction for multiple comparisons at $P < 0.05$.

After establishing the principal fiber direction of the significant cluster from the whole-brain FA correlation analysis, we performed probabilistic diffusion tractography (PROBTRACKX) in the control group only to identify the primary regions the cluster projects to. Tractography was initiated from the significant cluster and seed-based classification was performed using twelve cortical target masks covering the majority of frontal, motor, and sensory cortex, and fourteen subcortical target masks (cerebral peduncle, basal ganglia and thalamic subregions). For target mask details, see Supporting Information and Supporting Information Figure S2. All masks were transformed to subject diffusion space using the inverse of the registrations generated during TBSS. From each voxel in the seed mask 10,000 samples were generated with a curvature threshold of 0.2 and the number of samples reaching each of the cortical target masks was recorded. An exclusion mask was used to prevent tracts crossing the midline. For each voxel the probability of connecting to each cortical region was calculated as a proportion of the total number of samples from that voxel reaching any cortical area. In a separate analysis the same procedure was repeated for the subcortical target regions. Target regions with an average maximum connection probability >75th percentile were considered as having strong connectivity with the seed cluster. Finally, constrained probabilistic tractography between the relevant subcortical and cortical regions was performed in the control subjects. To determine the probable spatial trajectory of each tract, the maps representing the distribution of trajectories from seed to target were thresholded at a low level to remove noise (this was 0.02% of the maximum value in the connectivity map) transformed to MNI space (using the TBSS registrations), binarized, and summed across participants. Voxels that were present in >95% of control participants' maps were retained. The resulting MNI space tracts were used to extract the mean FA from each subjects' skeleton image generated during the TBSS analysis. Thus, the value for each tract can be thought to reflect the integrity of white matter projections to/from the nodes. Mean FA of each tract was correlated with switch cost to test for the linkage between structure and behavioral performance, controlling for mean skeleton FA and age (Statistica 8, StatSoft, Tulsa, OK). As a control analysis, we performed constrained probabilistic

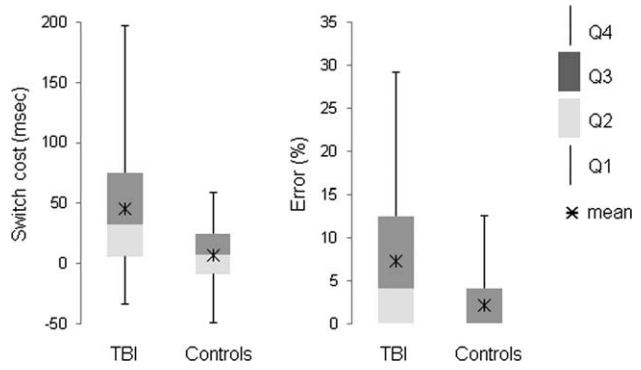

Figure 2.

Behavioral performance. Box-and-whisker diagram of local-global task performance. A) Switch cost (reaction time switch trials – repeat trials) for both groups. B) Errors on switch trials for both groups. Plots represent the group's smallest observation, the four quartiles (Q1–4), largest observation and the mean (x).

tractography between the middle frontal gyrus and intraparietal sulcus [superior longitudinal fasciculus (SLF)], between left and right supplementary motor complex [relevant part of corpus callosum (CC)], and between the cerebral peduncle and M_1 [corticospinal tract (CST)]. The reported P values are corrected for the number of comparisons using a modified Bonferroni correction [Holm, 1979].

RESULTS

TBI patients performed worse on both RT and accuracy measures (Fig. 2). Ten TBI patients deviated more than two SD's from the mean switch cost and/or switch accuracy of the control group (see Supporting Information Table SI). Switch cost was higher in TBI [$t(35) = 2.58$, $P = 0.007$, controls: 6.39 ± 28.00 ms, TBI: 45.32 ± 53.96 ms)] and patients made more errors while switching [$t(35) = 1.74$, $P = 0.045$, controls: $2 \pm 3.57\%$, TBI: $7 \pm 8.29\%$)] (Fig. 2).

The TBI group showed a widespread decline in FA throughout the TBSS skeleton compared to the healthy controls (Fig. 3). To examine the relationship between task switching and white matter integrity, we performed a TBSS regression analysis with switch cost as the variable of interest. To control for effects of processing speed on switch cost we added overall reaction time from the two unidimensional (nonswitch) task blocks as a covariate, as well as age. One cluster in right frontal white matter showed a significant negative relationship between FA and switch cost across all subjects (peak voxel $x, y, z = 19, -7, 42$; Fig 4A, yellow). The cluster was situated in an area with a high probability of crossing fibers. To disentangle these crossing fibers we estimated two scalars in each voxel, f_1 and f_2, associated with orientations $1\times$ and $2\times$, potentially indicating two different fiber populations within the voxel. After matching the partial volume fractions across subjects we performed a post hoc correlation analysis with switch cost. Only f_1 showed a significant negative correlation with switch cost (peak voxel $x, y, z = 19, -3, 43$). None of the voxels within the cluster ROI showed a significant relationship between switch cost and f_2. The negative correlation with switch cost is associated with the blue orientation in Figure 4A. These are fibers running dorsal-ventral as opposed to anterior-posterior/left-right (black orientation), indicating that the significant cluster from the whole-brain FA analysis likely

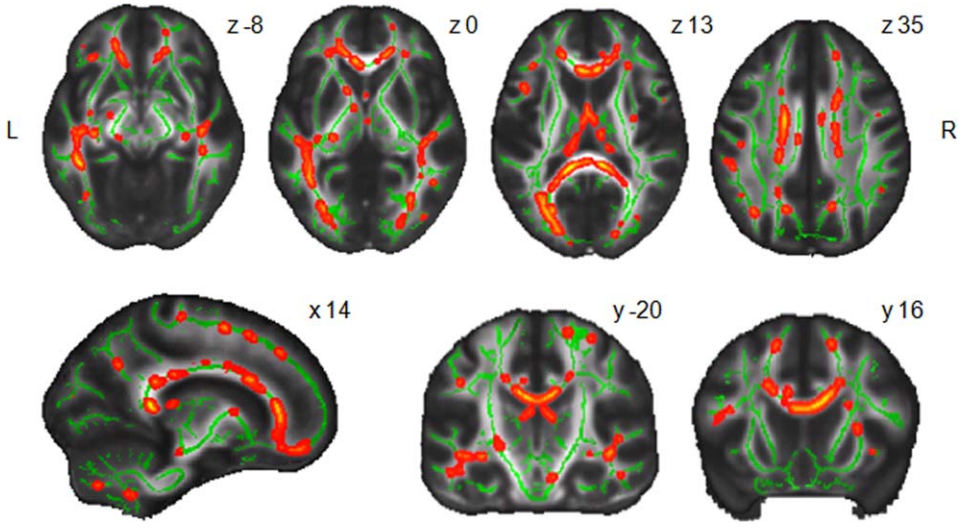

Figure 3.

Group differences in mean FA. Clusters with significantly reduced FA in the TBI group (cluster height threshold $t = 3.6$, $P < 0.05$) overlaid on the TBSS skeleton (green).

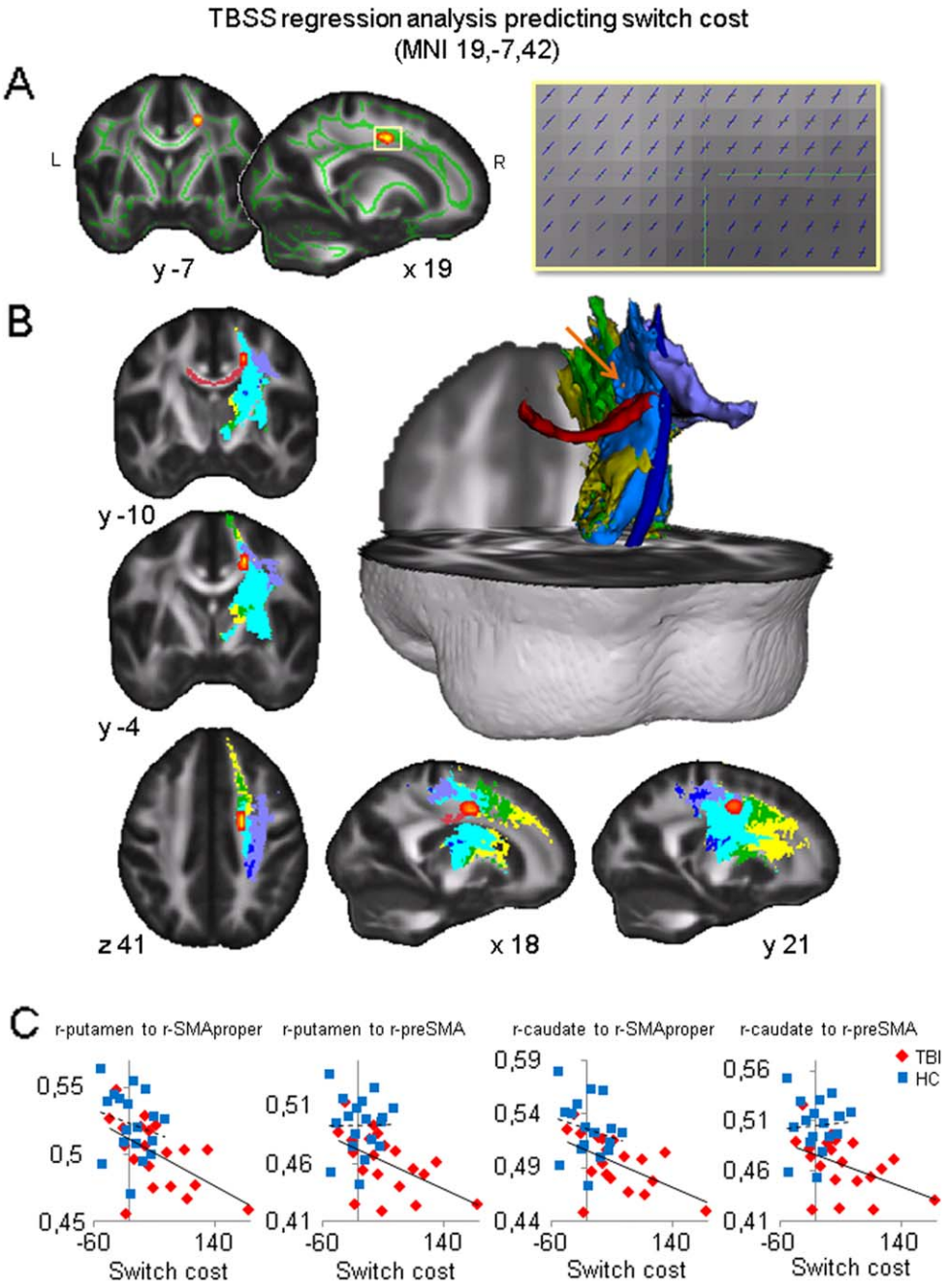

Figure 4.

Relationship between cortico-subcortical white matter and switch cost. (**A**) TBSS regression analysis result. Cluster in right white matter showing a significant negative correlation between FA and switch cost (cluster height threshold $t = 3.6$, $P < 0.05$) overlaid on the TBSS skeleton (green). The expanded ROI view shows the two distinct fiber populations present in the cluster (averaged across subjects). The negative correlation with switch cost is associated here with the blue orientations. (**B**) 3D rendering and slices of probabilistic tracts (>95% of control participants). Tracts are color coded as follows: Subcortical-SMAproper, light-blue; subcortical-preSMA, green; subcortical-SFG, yellow; CC, red; CST, blue; SLF, purple. Cluster with a significant negative correlation between FA and switch cost is overlaid on the tracts (red-yellow). (**C**) Correlations with switch cost and mean FA of probabilistic tracts from striatum to (pre-)SMA. Solid line = trend line TBI group, dashed line = trend line control group.

TABLE I. Reduced white matter integrity of cortico-subcortical connections and the relation with behavior

	TBI mean (SD)	Controls mean (SD)	*P*-value	Switch cost			Switch accuracy		
				All	TBI	HC	All	TBI	HC
Tracts									
r-putamen to r-SMAproper	0.50 (0.03)	0.52 (0.03)	0.007	**−0.53*****	**−0.69****	−0.46	0.29	0.20	0.35
r-putamen to r-preSMA	0.46 (0.03)	0.49 (0.03)	**<0.001**	**−0.57*****	**−0.74*****	−0.23	0.15	0.36	0.28
r-putamen to r-SFG	0.46 (0.03)	0.49 (0.03)	**0.001**	**−0.52****	**−0.72*****	−0.24	0.25	0.34	0.25
r-caudate to r-SMAproper	0.49 (0.03)	0.53 (0.03)	**<0.001**	**−0.51****	**−0.65****	−0.33	0.20	0.21	0.36
r-caudate to r-preSMA	0.47 (0.03)	0.51 (0.03)	**<0.001**	**−0.53*****	**−0.68****	−0.03	0.29	0.33	0.21
r-caudate to r-SFG	0.45 (0.03)	0.49 (0.03)	**<0.001**	**−0.49****	**−0.67****	−0.06	0.24	0.27	0.23
r-STN to r-SMAproper	0.56 (0.03)	0.57 (0.03)	0.095	−0.42	**−0.69****	−0.10	0.14	0.18	0.35
r-STN to r-preSMA	0.53 (0.03)	0.55 (0.03)	0.008	−0.43	**−0.70****	−0.07	0.24	0.38	0.17
r-STN to r-SFG	0.51 (0.03)	0.54 (0.03)	0.011	−0.42	**−0.64****	−0.24	0.18	0.30	0.18
r-thalamus to r-SMAproper	0.52 (0.03)	0.55 (0.03)	0.016	**−0.45****	−0.61	−0.28	0.12	0.13	0.34
r-thalamus to r-preSMA	0.55 (0.03)	0.58 (0.03)	0.012	−0.27	−0.53	0.003	0.18	0.26	0.21
r-thalamus to r-SFG	0.48 (0.03)	0.50 (0.03)	**0.003**	**−0.46*****	**−0.69****	−0.10	0.14	0.22	0.17
CC (SMC)	0.59 (0.06)	0.69 (0.04)	**<0.001**	−0.29	−0.20	−0.29	0.02	−0.09	−0.17
SLF (r-MFG to r-IPS)	0.48 (0.02)	0.49 (0.04)	0.27	−0.03	−0.38	0.04	−0.10	0.04	0.10
CST	0.50 (0.03)	0.51 (0.03)	0.22	−0.37	−0.60	−0.28	−0.11	−0.10	0.09
Control variables									
TBSS skeleton	0.41 (0.02)	0.45 (0.02)	**<0.001**	−0.31	−0.03	−0.15	0.35	0.18	0.17
Age	24.7 (5.6)	25.1 (1.9)	0.771	−0.05	−0.07	0.27	−0.06	−0.11	0.14
RT non-switch blocks	510.9 (63.2)	474.9 (46.3)	0.055	0.50	0.42	0.50			

Mean fractional anisotropy (FA) from ROI's determined using probabilistic tractography in the control group. Group differences in FA were examined using two-tailed, two-sample *t*-tests. Two-tailed Pearson's correlation coefficients are reported for the relationship between FA and behavior. The reported *P* values are corrected for the number of comparisons using a modified Bonferroni correction (bold) (Holm, 1979). *$P < 0.05$; **$P < 0.01$; ***$P < 0.001$. SMA = supplementary motor area, SFG = superior frontal gyrus, SMC = supplementary motor complex, STN = subthalamic nucleus, CC = corpus callosum, SLF = superior longitudinal fasciculus, MFG = middle frontal gyrus, IPS = intra-parietal sulcus, CST = corticospinal tract.

corresponds to the superior corona radiata, or possibly the corticospinal tract. The other fiber population could reflect the superior longitudinal fasciculus (SLF), or corpus callosum (CC). Figure 4B shows the overlap between the different tracts and the significant cluster.

The corona radiata contains both descending and ascending axons that carry nearly all neural traffic between subcortical and cortical regions. To identify which tracts run through the cluster, we selected 12 cortical regions and 14 subcortical regions as targets for probabilistic tractography with the cluster as a seed. The fibers running through the cluster connected most strongly to SMAproper, preSMA and superior frontal gyrus (SFG) (Supporting Information Fig. 3A). For the subcortical targets, it was impossible to differentiate between afferent and efferent connections, a known limitation of diffusion imaging [Jbabdi and Johansen-Berg. 2011]. The rostral motor zone of putamen, prefrontal zone of caudatus, STN, rostral motor and prefrontal zone of thalamus and the cerebral peduncle were most strongly connected with the cluster (Supporting Information Fig. 3B).

The correlation between switch cost and the mean FA values derived from the tracts running between these subcortical and cortical regions and the control tracts is shown in Table I and Figure 4C. Mean FA from the tracts between putamen, caudate, thalamus and (pre)-SMA and SFG were most predictive for switch cost across both groups and within the TBI group, whereas mean FA of CST, CC and SLF did not correlate significantly with switch cost.

A similar TBSS regression analysis predicting increased switching errors with decreased FA revealed clusters in left M_1 (peak voxel −13, −25, 63), right SMAproper (MNI 11, −3, 64), right external capsule (close to putamen, MNI 33, 11, −1) and the right posterior thalamic radiation (Fig. 5, Table I).

DISCUSSION

We used a partial volume model to disentangle crossing fibers for tract-based spatial statistics, enabling more tract specificity in the search for structural damage related to impairments in cognitive control over action in TBI. The results show that although patients had a widespread reduction in white matter mircostructural integrity, cortico-subcortical connections were the main contributors to switching deficits.

Cognitive outcome after TBI is highly variable, complicating prognosis [Lowenstein, 2009]. Overall, our TBI

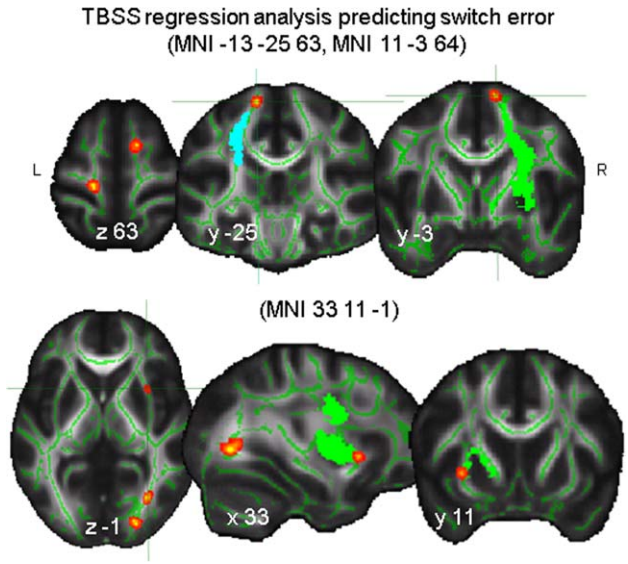

Figure 5.

Relationship between white matter and switch accuracy. TBSS regression analysis predicting switch accuracy. Significant clusters in which lower FA is associated with more switch errors (cluster height threshold $t = 3.6$, $P < 0.05$) overlaid on the TBSS skeleton (green). Clusters are dilated by two voxels to improve visualization.

patients performed worse on the local-global task, but there was a high degree of variability among patients (Fig. 2). Variation in task-relevant white matter tract integrity can partially explain individual behavioral differences in healthy adults [Johansen-Berg, 2010; Kanai and Rees, 2011] and normal aging [Grieve et al., 2007; Gold et al., 2010]. DAI may exacerbate such variation and account for the task switching impairments in TBI. The correlation between switch cost and FA of the frontal-subcortical circuits indeed suggests that DAI disrupts cortico-subcortical connectivity, limiting the ability to enforce efficient cognitive control over action.

Although less susceptible to direct contusion, the subcortical structures are sensitive to damage due to their extensive connections with the cortex. The highest stress shear concentration has been reported for thalamus and midbrain [Zhang et al., 2004]. Each thalamic nucleus has a distinct cortical connectivity pattern [Johansen-Berg et al., 2005], and lesions to the paramedian part of the thalamus have been shown to result in executive dysfunction [Van der Werf et al., 2000; Carrera and Bogousslavsky, 2006; Little et al., 2010]. Traditionally the BG have been associated with movement control, but antero- and retrograde labeling studies in animals indicated that the BG are also connected to the prefrontal cortex [Alexander et al., 1990]. Moreover, neuropsychological studies in patients with Parkinson's and Huntington's disease have shown that the BG indeed contribute to a variety of executive functions [Taylor and Saintcyr 1995; Brandt and Butters 1996]. Subsequently, the evidence for a functional role of the BG in cognitive control over action has accumulated [Graybiel, 2005; Monchi et al., 2006]. It is interesting to note that the TBI patients performing outside the two SD range of the control group, predominantly showed evidence of DAI, in terms of microbleeds in the frontal cortex and/or subcortical structures, as opposed to frontal lobe contusions (see Supporting Information Table SI).

Previous studies exploring the relationship between white matter structure and executive function in TBI generally used a region of interest approach, limiting the analysis to a priori selected white matter tracts [Kraus et al., 2007; Niogi et al., 2008; Lipton et al., 2009]. As white matter damage is diffuse in TBI, whole brain statistics seem more appropriate. Placement of regions of interest requires a priori knowledge of the likely location of the effects of interest, which is both difficult and restrictive. Whole brain tract-based spatial statistics have been used in this context [Kinnunen et al., 2011], but the results can be difficult to interpret, especially in regions with crossing fibers. Here, we modeled the diffusion signal as a weighted sum of signals accounting for the contribution of various compartments in each voxel. Such a partial volume model can enhance interpretability by providing more tract specific information [Jbabdi et al., 2010]. The relationship between executive dysfunction in TBI and structural integrity of the corona radiata has been described before [Kraus et al., 2007; Niogi et al., 2008; Bonnelle et al., 2012]. The results also add to a recent study from Little et al. [2010], which showed that FA from fibers running from thalamic seed voxels was related to executive function, attention and memory. Here, we extend these observations by identifying the specific frontal-subcortical connections within the corona radiata that affect switching performance. We provide additional specificity by demonstrating that the relationship between switch cost and FA in the neighboring tracts, CST, SLF, and CC, is not significant. The emerging perspective is that executive dysfunction is caused by cortico-subcortical damage rather than simply due to damage to the frontal lobe or cortico-cortical tracts.

Cortico-basal ganglia networks have been shown to play a role in higher-order threshold adjustment processes during switching [Mansfield et al., 2011]. In a healthy brain, preSMA can bias striatum to set an appropriate degree of conservativeness for a repetition or switch trial, creating an appropriate balance between speed and accuracy. However, when the connections between SMA and striatum are compromised, a tight control over this response threshold might not be possible [Forstmann et al., 2011]. Damage to cortico-striatal connections might have forced some of the TBI patients to shift their response threshold to a "safer" zone, slowing down in reaction time but preserving an acceptable level of accuracy.

Switching errors significantly correlated with reduced FA in left M_1, right SMAproper and the external capsule close to putamen. This might suggest that switching errors are more related to regions involved in movement

execution rather than regions involved in movement planning and reprogramming.

DTI is able to pick up on diffuse axonal injuries on a group level, and the specificity of the location of these injuries can be greatly improved by using a crossing fiber model. However, as pointed out earlier, TBI is a heterogeneous condition, and to use DTI in a clinical setting requires a personalized approach that allows comparison between individual DTI metrics and normative values with a minimal amount of postprocessing steps [Shenton et al., 2012]. Techniques like pattern classifiers seem promising [Hellyer et al., 2012]. Optimization would require an extensive map of human brain circuitry of a large number of subjects. Initiatives like the Human Connectome Project (www.humanconnectome.org) might eventually help to achieve an individual profile of injury. In the mean time, we should try to find solutions for the technical limitations of DTI [Jbabdi and Johansen-Berg, 2011], and we should acquire more knowledge about the functional implication of damage to specific tracts.

To summarize, our findings highlight the importance of considering frontal-subcortical circuits in neural models of executive control in TBI. Rather than focusing on damage to the frontal lobe, the connections between cortical and subcortical regions that ensure transmission of information across these remote areas should be taken into account [Caeyenberghs et al., 2012]. Using a whole-brain approach to identify the regions that are essential for successful task performance, and carefully investigating to which fiber population these white matter regions can be ascribed, can lead to a better understanding of the pathophysiology of TBI.

ACKNOWLEDGMENTS

The authors thank Monique Geurts from the Movement Control and Neuroplasticity Research Group of the KU Leuven for assistance with data collection.

REFERENCE

Alexander GE, Crutcher MD, DeLong MR (1990): Basal ganglia-thalamocortical circuits: Parallel substrates for motor, oculomotor, "prefrontal" and "limbic" functions. Prog Brain Res 85:119–146.

Arfanakis K, Haughton VM, Carew JD, Rogers BP, Dempsey RJ, Meyerand ME (2002): Diffusion tensor MR imaging in diffuse axonal injury. Am J Neuroradiol 23:794–802.

Basser PJ (1995): Inferring microstructural features and the physiological state of tissues from diffusion-weighted images. NMR Biomed 8:333–344.

Behrens TEJ, Berg HJ, Jbabdi S, Rushworth MFS, Woolrich MW (2007): Probabilistic diffusion tractography with multiple fibre orientations: What can we gain? Neuroimage 34:144–155.

Behrens TEJ, Woolrich MW, Jenkinson M, Johansen-Berg H, Nunes RG, Clare S, Matthews PM, Brady JM, Smith SM (2003): Characterization and propagation of uncertainty in diffusion-weighted MR imaging. Magn Reson Med 50:1077–1088.

Bhatia KP, Marsden CD (1994): The behavioral and motor consequences of focal lesions of the basal ganglia in man. Brain 117: 859–876.

Bianchi L (1985): The functions of the frontal lobes. Brain 18:497–522.

Bigler ED (2001): The lesion(s) in traumatic brain injury: Implications for clinical neuropsychology. Arch Clin Neuropsychol 16: 95–131.

Bonnelle V, Ham TE, Leech R, Kinnunen KM, Mehta MA, Greenwood RJ, Sharp DJ (2012): Salience network integrity predicts default mode network function after traumatic brain injury. Proc Natl Acad Sci USA 109:4690–4695.

Brandt J, Butters N (1996):Neuropsychological characteristics of Huntington's disease. In:Grant L, Adams KM, Editors. Neuropsychological Assesment of Neuropsychiatric Disorders. New York: Oxford University Press. pp 312–341.

Buki A, Povlishock JT (2006): All roads lead to disconnection? Traumatic axonal injury revisited. Acta Neurochir 148:181–193.

Caeyenberghs K, Leemans A, Heitger MH, Leunissen I, Dhollander T, Sunaert S, Dupont P, Swinnen SP (2012): Graph analysis of functional brain networks for cognitive control of action in traumatic brain injury. Brain 135:1293–1307.

Carrera E, Bogousslavsky J (2006): The thalamus and behavior - Effects of anatomically distinct strokes. Neurology 66:1817–1823.

Colantonio A, Ratcliff G, Chase S, Kelsey S, Escobar M, Vernich L (2004): Long-term outcomes after moderate to severe traumatic brain injury. Disabil Rehabil 26:253–261.

Draper K, Ponsford J (2008): Cognitive functioning ten years following traumatic brain injury and rehabilitation. Neuropsychol 22:618–625.

Forstmann BU, Tittgemeyer M, Wagenmakers EJ, Derrfuss J, Imperati D, Brown S (2011): The speed-accuracy tradeoff in the elderly brain: A structural model-based approach. J Neurosci 31:17242–17249.

Gentry LR, Godersky JC, Thompson B (1988): MR imaging of head trauma: Review of the distribution and radiopathologic features of traumatic lesions. AJR Am J Roentgenol 150:663–672.

Gold BT, Powell DK, Xuan L, Jicha GA, Smith CD (2010): Age-related slowing of task switching is associated with decreased integrity of frontoparietal white matter. Neurobiol Aging 31: 512–522.

Graybiel AM (2005): The basal ganglia: Learning new tricks and loving it. Curr Opin Neurobiol 15:638–644.

Grieve SM, Williams LM, Paul RH, Clark CR, Gordon E (2007): Cognitive aging, executive function, and fractional anisotropy: A diffusion tensor MR imaging study. Am J Neuroradiol 28:226–235.

Hellyer PJ, Leech R, Ham TE, Bonnelle V, Sharp DJ (2012): Individual prediction of white matter injury following traumatic brain injury. Ann Neurol.

Hikosaka O, Isoda M (2010): Switching from automatic to controlled behavior: Cortico-basal ganglia mechanisms. Trends Cog Sci 14:154–161.

Holm S (1979): A simple sequentially rejective multiple test procedure. Scandinavian Journal of Statistics 6:65–70.

Jbabdi S, Behrens TEJ, Smith SM (2010): Crossing fibres in tract-based spatial statistics. Neuroimage 49:247–256.

Jbabdi S, Johansen-Berg H (2011): Tractography: Where do we go from here? Brain Connect 1:169–183.

Johansen-Berg H (2010): Behavioural relevance of variation in white matter microstructure. Curr Opin Neurobiol 23:351–358.

Johansen-Berg H, Behrens TEJ, Sillery E, Ciccarelli O, Thompson AJ, Smith SM, Matthews PM (2005): Functional-anatomical validation and individual variation of diffusion tractography-based segmentation of the human thalamus. Cereb Cortex 15: 31–39.

Kanai R, Rees G (2011): The structural basis of inter-individual differences in human behaviour and cognition. Nat Rev Neurosci 12:231–242.

Kinnunen KM, Greenwood R, Powell JH, Leech R, Hawkins PC, Bonnelle V, Patel MC, Counsell SJ, Sharp DJ (2011): White matter damage and cognitive impairment after traumatic brain injury. Brain 134:449–463.

Kraus MF, Susmaras T, Caughlin BP, Walker CJ, Sweeney JA, Little DM (2007): White matter integrity and cognition in chronic traumatic brain injury: A diffusion tensor imaging study. Brain 130:2508–2519.

Krause M, Mahant N, Kotschet K, Fung VS, Vagg D, Wong CH, Morris JGL (2012): Dysexecutive behaviour following deep brain lesions—A different type of disconnection syndrome? Cortex 48:97–119.

Larson MJ, Perlstein WM, Demery JA, Stigge-Kaufman DA (2006): Cognitive control impairments in traumatic brain injury. J Clin Exp Neuropsychol 28:968–986.

Leunissen I, Coxon JP, Geurts M, Caeyenberghs K, Michiels K, Sunaert S, Swinnen SP (2013): Disturbed cortico-subcortical interactions during motor task switching in traumatic brain injury. Hum Brain Mapp 34:1254–1271.

Levin HS, Hanten G, Zhang LF, Swank PR, Hunter J (2004): Selective impairment of inhibition after TBI in children. J Clin Exp Neuropsychol 26:589–597.

Levy R, Dubois B (2006): Apathy and the functional anatomy of the prefrontal cortex-basal ganglia circuits. Cereb Cortex 16: 916–928.

Lipton ML, Gulko E, Zimmerman ME, Friedman BW, Kim M, Gellella E, Gold T, Shifteh K, Ardekani BA, Branch CA (2009): Diffusion-tensor imaging implicates prefrontal axonal injury in executive function impairment following very mild traumatic brain injury. Radiology 252:816–824.

Little DM, Kraus MF, Joseph J, Geary EK, Susmaras T, Zhou XJ, Pliskin N, Gorelick PB (2010): Thalamic integrity underlies executive dysfunction in traumatic brain injury. Neurology 74: 558–564.

Lowenstein DH (2009): Traumatic brain injury: A glimpse of order among the chaos? Ann Neurol 66:A7–A8.

Mac Donald CL, Dikranian K, Bayly P, Holtzman D, Brody D (2007): Diffusion tensor imaging reliably detects experimental traumatic axonal injury and indicates approximate time of injury. J Neurosci 27:11869–11876.

Malec JF, Brown AW, Leibson CL, Flaada JT, Mandrekar JN, Diehl NN, Perkins PK (2007): The Mayo classification system for traumatic brain injury severity. J Neurotrauma 24:1417–1424.

Mansfield EL, Karayanidis F, Jamadar S, Heathcote A, Forstmann BU (2011): Adjustments of response threshold during task switching: A model-based functional magnetic resonance imaging study. J Neurosci 31:14688–14692.

Mecklinger AD, von Cramon DY, Springer A, Matthes-von CG (1999): Executive control functions in task switching: Evidence from brain injured patients. J Clin Exp Neuropsychol 21:606–619.

Mink JW (1996): The basal ganglia: Focused selection and inhibition of competing motor programs. Prog Neurobiol 50:381–425.

Miyake A, Friedman NP, Emerson MJ, Witzki AH, Howerter A, Wager TD (2000): The unity and diversity of executive functions and their contributions to complex "frontal lobe" tasks: A latent variable analysis. Cogn Psychol 41:49–100.

Monchi O, Petrides M, Strafella AP, Worsley KJ, Doyon J (2006): Functional role of the basal ganglia in the planning and execution of actions. Ann Neurol 59:257–264.

Nachev P, Kennard C, Husain M (2008): Functional role of the supplementary and pre-supplementary motor areas. Nat Rev Neurosci 9:856–869.

Nambu A, Tokuno H, Takada M (2002): Functional significance of the cortico-subthalamo-pallidal 'hyperdirect' pathway. Neurosci Res 43:111–117.

Navon D (1977): Forest before trees—Precedence of global features in visual-perception. Cogn Psychol 9:353–383.

Newcombe VF, Outtrim JG, Chatfield DA, Manktelow A, Hutchinson PJ, Coles JP, Williams GB, Sahakian BJ, Menon DK (2011): Parcellating the neuroanatomical basis of impaired decision-making in traumatic brain injury. Brain 134:759–768.

Niogi SN, Mukherjee P, Ghajar J, Johnson C, Kolster RA, Sarkar R, Lee H, Meeker M, Zimmerman RD, Manley GT, McCandliss BD (2008): Extent of microstructural white matter injury in postconcussive syndrome correlates with impaired cognitive reaction time: A 3T diffusion tensor imaging study of mild traumatic brain injury. Am J Neuroradiol 29:967–973.

Oldfield RC (1971): Assessment and analysis of handedness—Edinburgh inventory. Neuropsychologia 9:97–113.

Perlstein WM, Larson MJ, Dotson VM, Kelly KG (2006): Temporal dissociation of components of cognitive control dysfunction in severe TBI: ERPs and the cued-Stroop task. Neuropsychologia 44:260–274.

Rugg-Gunn FJ, Symms MR, Barker GJ, Greenwood R, Duncan JS (2001): Diffusion imaging shows abnormalities after blunt head trauma when conventional magnetic resonance imaging normal. J Neurol Neurosurg Psychiatry 70:530–533.

Rushworth MFS, Walton ME, Kennerley SW, Bannerman DM (2004): Action sets and decisions in the medial frontal cortex. Trends Cog Sci 8:410–417.

Scheid R, Preul C, Gruber O, Wiggins C, von Cramon DY (2003): Diffuse axonal injury associated with chronic traumatic brain injury: Evidence from T2*-weighted gradient-echo imaging at 3 T. Am J Neuroradiol 24:1049–1056.

Seignourel PJ, Robins DL, Larson MJ, Demery JA, Cole M, Perlstein WM (2005): Cognitive control in closed head injury: Context maintenance dysfunction or prepotent response inhibition deficit? Neuropsychol 19:578–590.

Shenton ME, Hamoda HM, Schneiderman JS, Bouix S, Pasternak O, Rathi Y, Vu MA, Purohit MP, Helmer K, Koerte I, Lin AP, Westin CF, Kikinis R, Kubicki M, Stern RA, Zafonte R (2012): A review of magnetic resonance imaging and diffusion tensor imaging findings in mild traumatic brain injury. Brain Imaging Behav 6:137–192.

Smith SM, Jenkinson M, Johansen-Berg H, Rueckert D, Nichols TE, Mackay CE, Watkins KE, Ciccarelli O, Cader MZ, Matthews PM, Behrens TEJ (2006): Tract-based spatial statistics: Voxelwise analysis of multi-subject diffusion data. Neuroimage 31:1487–1505.

Tagliaferri F, Compagnone C, Korsic M, Servadei F, Kraus J (2006): A systematic review of brain injury epidemiology in Europe. Acta Neurochir 148:255–268.

Taylor AE, Saintcyr JA (1995): The neuropsychology of Parkinsons-disease. Brain Cogn 28:281–296.

Tournier JD, Mori S, Leemans A (2011): Diffusion tensor imaging and beyond. Magn Reson Med 65:1532–1556.

Van der Werf YD, Witter MP, Uylings HBM, Jolles J (2000): Neuropsychology of infarctions in the thalamus: A review. Neuropsychologia 38:613–627.

Wallesch CW, Curio N, Galazky I, Jost S, Synowitz H (2001a): The neuropsychology of blunt head injury in the early postacute stage: Effects of focal lesions and diffuse axonal injury. J Neurotrauma 18:11–20.

Wallesch CW, Curio N, Kutz S, Jost S, Bartels C, Synowitz H (2001b): Outcome after mild-to-moderate blunt head injury: Effects of focal lesions and diffuse axonal injury. Brain Injury 15: 401–412.

Zappala G, Thiebaut de Schotten M, Eslinger PJ (2012): Traumatic brain injury and the frontal lobes: What can we gain with diffusion tensor imaging? Cortex 48:156–165.

Zhang L, Plotkin RC, Wang G, Sandel ME, Lee S (2004): Cholinergic augmentation with donepezil enhances recovery in short-term memory and sustained attention after traumatic brain injury. Arch Phys Med Rehabil 85:1050–1055.